CoMFA and CoMSIA studies on a series of fluroquinolone derivatives for potential anti-inflammatory activity

4 AUTHORS, INCLUDING:

Asia Naz
University of Karachi
17 PUBLICATIONS 63 CITATIONS

SEE PROFILE

Zaheer Ulhaq
University of Karachi
101 PUBLICATIONS 941 CITATIONS

SEE PROFILE

Farhan Ahmed Siddiqui
University of Karachi
67 PUBLICATIONS 331 CITATIONS

SEE PROFILE

PAPER

CrossMark
click for updates

CoMFA and CoMSIA studies on a series of fluroquinolone derivatives for potential anti-inflammatory activity

Asia Naz,[a] Hina Shamshad,[b] Zaheer ul Haq[b] and Farhan Ahmed Siddiqui*[cd]

Three-dimensional quantitative structure–activity relationships using CoMFA and CoMSIA were developed for a series of 28 fluroquinolone derivatives for prediction of anti-inflammatory activity. QSAR models with high squared correlation coefficients of up to 0.962 for CoMFA, 0.989 for CoMSIA-I and 0.987 for CoMSIA-II were established. The robustness of the model was confirmed with the help of leave-one-out cross-validation having values of 0.554 for CoMFA, 0.6 for CoMSIA-I and 0.597 for CoMSIA-II, respectively. Theoretical results were in accordance with the experimental data. Developed models highlighted the importance of steric, electrostatic, hydrophobic and donor descriptors for anti-inflammatory activity.

Introduction

Fluoroquinolones are potent antibiotics with a broad antibacterial spectrum.[1] Antibacterial activity of fluroquinolones is due to their ability to interfere with the replication of bacterial DNA. Recently, it has been discovered that some new fluroquinolones act against topoisomerase II and also inhibit synthesis of the pro-inflammatory cytokines IL-8, TNF-α and IL-lb. Furthermore, they showed cytotoxic and anti-inflammatory activities too.[2,3] Therefore, in addition to their antimicrobial properties, these drugs were found to possess anti-inflammatory activities also, which were investigated, and some fluroquinolones showed bifunctional activities.[4–6]

Thus, in order to correlate anti-inflammatory activity with the structure of quinolone derivatives, for the first time a 3D quantitative structure–activity relationship (QSAR) model was developed and validated. 3D-QSAR has become an integral part of ligand-based drug discovery and design.[7] There are a number of QSAR models for predicting the antibacterial activity of fluoroquinolone, which revealed that N1, C2-H, C3-carboxylic acid, C4-carbonyl, C6-F, and C7-piperazine are beneficial for the anti-bacterial activity.[8–10] However, there was not a single QSAR model to predict the anti-inflammatory activity of fluroquinolone. The identification of structural features responsible for the anti-inflammatory activity of fluroquinolone can pave the way for the design of fluroquinolone compounds with a good anti-inflammatory activity.

Comparative Molecular Field Analysis (CoMFA)[11] and Comparative Molecular Similarity Indices Analysis (CoMSIA)[12] are two of the most widely accepted QSAR models. In CoMFA, the biological activities of compounds are linked with electrostatic and steric properties[13,14] and require the conditions both for the alignments and conformations of molecules. As a complementary technique, CoMSIA calculates hydrophobic and hydrogen-bond donor and acceptor indices in addition to electrostatic and steric indices.[15]

In the present study, 3D-QSAR models using CoMFA and CoMSIA for the anti-inflammatory activity of fluroquinolone derivatives were developed. These models were validated by leave one out cross validation.[16,17] The models were further validated for their regression coefficient, internal and external predictive ability and statistical significance.[18] This study can serve as a basis in guiding the synthetic chemist to search for new compounds possessing an enhanced anti-inflammatory activity along with antimicrobial activities.

Infection is a pathological progression whereby any exogenous mediator (fungus, bacterium or virus) assaults the body, causing some form of ruinous dysfunction. Upon an infection of microorganisms, inflammatory cytokines (such as TNF-α) are formed from macrophages and can lead to a variety of conditions such as autoimmune, allergic, and inflammatory diseases,[19] such as cystic fibrosis, which is characterized by chronic neutrophilic inflammation.[20,21] These types of diseases are obligatorily treated with a combination of immune system-harmless anti-inflammatory and antimicrobial agents. Fluoroquinolones have long been used as antimicrobial therapy in urinary, respiratory, sexual and GI infections.[22] A number of studies have shown that new fluoroquinolones also possess immunomodulatory properties beyond their antimicrobial

[a]*Research Institute of Pharmaceutical Sciences, Department of Pharmaceutical Chemistry, Faculty of Pharmacy, University of Karachi, Pakistan*

[b]*Dr Panjwani Centre for Molecular Medicine and Drug Research, International Centre for Chemical and Biological Sciences, University of Karachi, Pakistan*

[c]*Faculty of Pharmacy, Federal Urdu University Arts, Science and Technology, Karachi 75300, Pakistan. E-mail: farhanchemist@gmail.com*

[d]*Faculty of Pharmacy, Ziauddin University, Karachi, Pakistan*

effects.[23] Gatifloxacin sesquihydrate, a broad-spectrum antimicrobial fluoroquinolone,[24–27] also has an inhibitory effect on the production of inflammatory cytokines by macrophages, monocytes or peripheral lymphocytes and mainly suppresses bacterial infection-induced inflammation.[28,29] On the basis of the anti-inflammatory activity of fluoroquinolones, our initial efforts for new anti-inflammatory agents included the structural modification of fluoroquinolones in an anticipation of the preservation of the antibacterial activity with an enhancement of its anti-inflammatory activity.

Experimental

Energy minimization and alignment of molecules

The series of compounds reported by Najma *et al.*,[28] were used to derive 3D-QSAR models. The chemical structures of molecules and their experimental anti-inflammatory (IC_{50}) values are shown in Table 1. The 2D structures of fluroquinolone derivatives were constructed using ChemDraw version 64-1.5.3 (ref. 30) and converted into 3D by MOE (Molecular Operating Environment) program.[31] Then, compounds were filtered and assigned Gasteiger–Hückel charge. These compounds were optimized for energy minimization using MMFF94 (Merck Molecular Force Field) using SYBL 7.3 software. The threshold value for root mean square (RMS) gradient was kept at 0.001 kcal mol^{-1} Å^{-1}. All molecules were subsequently aligned by a template-based alignment technique using a common structure as a template.[32] The most active compound, no. **27**, was selected as a template for the alignment of molecules. All the compounds aligned well to compound **27**, as shown in Fig. 1. The alignment is useful for studying shape variation with respect to the base structure selected for alignment.[33–35]

Design of the training and test sets

A QSAR model attempts to find consistent relationships between the variations in the values of molecular properties and anti-inflammatory activity for a series of compounds, which can then be used to evaluate the properties of new chemical entities.[36] The derivatives were randomly divided into a training set and test set comprising **23** and **5** compounds, respectively.

CoMFA and CoMSIA 3D-QSAR model

CoMFA and CoMSIA analyses were performed using SYBYL version 7.3 (Tripos, Inc., St. Louis, MO) running on a Silicon Graphics Fuel workstation with the IRIX 6.5 operating system. In both CoMFA and CoMSIA analyses, 3D cubic lattice with a grid spacing of 2 Å was created to encompass the aligned molecules.[11] The SYBYL default cutoff of 30 kcal mol^{-1} was used for field energy calculations. The CoMFA and CoMSIA descriptors were used as independent variables, and pK_i values were used as dependent variables to derive 3D QSAR models. The predictive value of the models was evaluated by cross validation. The optimal number of components was determined by selecting the smallest PRESS value. Usually, this value corresponds to the highest q^2 value and was subsequently used to derive the final QSAR models. In addition to q^2, the

corresponding PRESS, the number of components, the conventional correlation coefficient (r^2), and its standard error (s) were also computed.

Results and discussion

CoMFA analysis

Partial Least Squares regression (PLS) analysis of the training set gave a cross-validated q^2 value of 0.554 with an optimum component number of 6. The non-cross-validated PLS analysis was repeated with the optimum number of components, to give an r^2 of 0.962, $F(6, 16) = 67.63$ (Fisher ratio), and an estimated standard error of 0.172, as shown in Table 2. The steric descriptors showed 48.1% variance, while the electrostatic descriptors gave 51.9% variance, as is obvious from Table 2. According to the Tropsha group,[37] a QSAR model is considered predictive if the following conditions are satisfied:

$$q^2 > 0.5r^2 > 0.6$$

or

$$r^2 - r_0^2/-r^2 \text{ is less than } 0.1k \text{ or } k \text{ is close to } 1$$

where r^2 is the coefficient of determination between experimental values and model prediction on the training set.[37] The proposed CoMFA model passed all these tests with respect to predictive ability.

$$r_{cv}^2 > 0.554 > 0.5r^2 = 0.962 > 0.6$$

$$r^2 - r_0^{'2}/r^2 = 0.00 < 0.1k = 0.99$$

The predicted activities *versus* their experimental activities are listed in Table 3. The correlation between the predicted activities and the experimental activities is depicted in Fig. 2A. Tables 2 and 3 and Fig. 2A demonstrate that the predicted activities of the CoMFA model are in good agreement with the experimental data.

CoMSIA analysis

Forty different CoMSIA models were constructed to correlate the anti-inflammatory activity with physiochemical properties such as steric, electrostatic, hydrophobic, hydrogen-bond donor and acceptor. The two best models, CoMSIA-I and CoMSIA-II, were selected on the basis of the q^2 values. CoMSIA-I was performed using two descriptor fields: steric and hydrophobic with q^2 (cross validated r^2) value of 0.6, optimum component number of 6. The non-cross-validated PLS analysis was found to have r^2 of 0.989, $F = 234.231$ and an estimated standard error of 0.094 as shown in Table 2. CoMSIA-II was performed using five descriptor fields: steric, electrostatic, hydrophobic, hydrogen-bond donor and acceptor. PLS analysis was performed, with a q^2 value of 0.597, component number of 6, non-cross-validated r^2 of 0.987, $F = 27.151$, and an estimated standard error of 0.10. These values clearly indicated that a better statistical

Table 1 Chemical structure and K_i values (IC$_{50}$) of the fluroquinolone derivatives used to generate the QSAR prediction model[3,4,19]
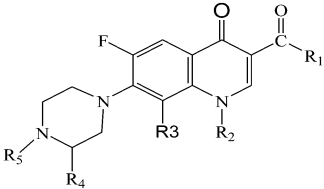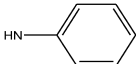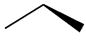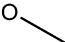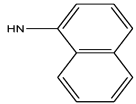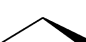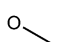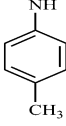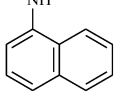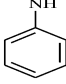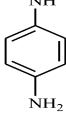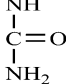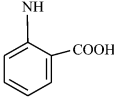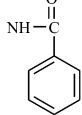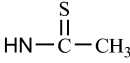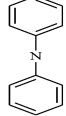

Compound	R$_1$	R$_2$	R$_3$	R$_4$	R$_5$	IC$_{50}$ (µg ml^{-1})
1	OH	△	OCH$_3$	CH$_3$	H	31
2	HN–phenyl		O–ethyl	H	CH$_3$	12.3
3	HN–naphthyl		O–ethyl	H	CH$_3$	13.1
4	NH–C$_6$H$_4$–CH$_3$	△	OCH$_3$	CH$_3$	H	110
5	NH–naphthyl	△	OCH$_3$	CH$_3$	H	9.7
6	NH–phenyl	△	OCH$_3$	CH$_3$	H	39.3
7	NH–C$_6$H$_4$–NH$_2$	△	OCH$_3$	CH$_3$	H	6.3
8	NH–C(=O)–NH$_2$	△	OCH$_3$	CH$_3$	H	34.6
9	NH–C$_6$H$_4$–COOH	△	OCH$_3$	CH$_3$	H	202
10	NH–C(=O)–phenyl	△	OCH$_3$	CH$_3$	H	69.6
11	HN–C(=S)–CH$_3$	△	OCH$_3$	CH$_3$	H	239
12	N(phenyl)$_2$	△	OCH$_3$	CH$_3$	H	949
13	NHNH$_2$	△	OCH$_3$	CH$_3$	H	90.7

Table 1 (Contd.)
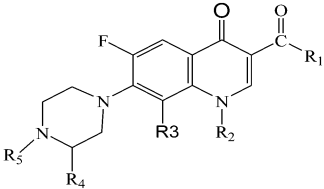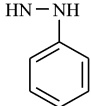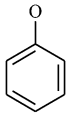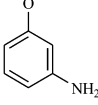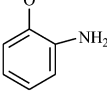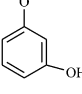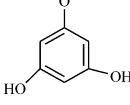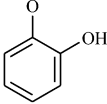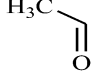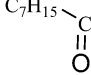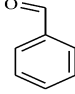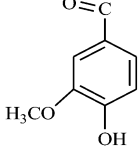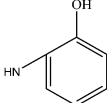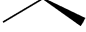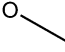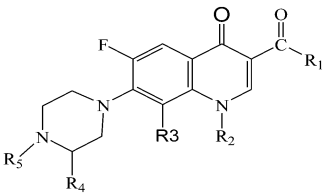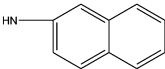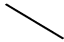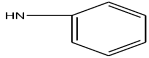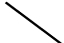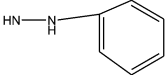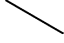
Compound	R_1	R_2	R_3	R_4	R_5	IC_{50} ($\mu g\ ml^{-1}$)
14			OCH_3	CH_3	H	21.5
15			OCH_3	CH_3	H	10.8
16			OCH_3	CH_3	H	6.7
17			OCH_3	CH_3	H	7.9
18			OCH_3	CH_3	H	135.6
19			OCH_3	CH_3	H	73.6
20			OCH_3	CH_3	H	9.9
21	OH		OCH_3	CH_3		240
22	OH		OCH_3	CH_3		8.43
23	OH		OCH_3	CH_3		238
24	OH		OCH_3	CH_3		245
25				H	CH_3	8.5

Table 1 (Contd.)

Compound	R$_1$	R$_2$	R$_3$	R$_4$	R$_5$	IC$_{50}$ (μg ml^{-1})
26	HN— (naphthalene)	—	H	H	H	2.6
27	HN— (phenyl)	—	H	H	H	1.4
28	HN—NH (phenylhydrazine)	—	H	H	H	13.3

Fig. 1 Database alignment used in 3D-QSAR studies with compound 27 as the template ligand.

correlation was achieved in CoMSIA-I in comparison to that in CoMSIA-II. However, both the proposed CoMSIA models passed the tests of predictive ability described earlier.

$$r_{cv}^2 > 0.6 > 0.5 r^2 = 0.989 > 0.6 \text{ (analysis I)}$$

$$r^2 - r_0'^2 / - r^2 = 0.00 < 0.1 k = 0.99$$

$$r_{cv}^2 > 0.597 > 0.5 r^2 = 0.987 > 0.6 \text{ (analysis II)}$$

$$r^2 - r_0'^2 / - r^2 = 0.00 < 0.1 k = 0.99$$

As is obvious from Table 2, the percentage of the variance explained by steric and hydrophobic field descriptors are 53 and 45.7% in case of CoMSIA-I analysis, while in the case of CoMSIA-II contribution of steric, electrostatic, hydrophobicity, hydrogen-bond donor and hydrogen-bond acceptor field descriptors are 0.8, 30.3, 30.3, 28.7 and 0%, respectively. The predicted anti-inflammatory activities are listed in Table 3. The correlations between the experimental and predicted bioactivities are shown in Fig. 2B and C.

Table 2 Statistical indices of CoMFA and CoMSIA models

Parameter	CoMFA	CoMSIA (I)	CoMSIA (II)
q^2	0.554	0.6	0.597
Component	0.6	0.6	0.6
SEE	0.172	0.094	0.100
r^2	0.962	0.989	0.987
F	67.63 (6, 16)	234.231	207.151
r_{prob}^2	0.000	0.000	0.000
% Contribution			
Steric	0.481	0.533	0.108
Electrostatic	0.519	—	0.303
Hydrophobic	—	0.457	0.303
Hydrogen bond donor	—	—	0.287
Hydrogen bond acceptor	—	—	—

Model validation

The CoMFA and CoMSIA models' predictive activities were verified by the five molecules of the test set, as depicted in Table 1. The predicted pIC$_{50}$ values were in good agreement with the experimental pIC$_{50}$ values, having very small functional differences. The predicted r^2 value was 0.781 and 0.583 for CoMFA and CoMSIA, respectively, as shown in Table 2 (Fig. 2A–C). The results clearly indicated the reliability of the models for the activity predictions of new compounds.

Contour analysis

The visualization of the results of the CoMFA and CoMSIA models have been performed using the StDev*Coeff mapping option contoured by contribution. The default level of contour by contribution, 90 for favored region and 10 for disfavored region, was set during contour analysis.

Table 3 Compound with observed and calculated pK_i values[a]

	pK_i	Predicted			Residual		
	Observed	CoMFA	CoMSIA (I)	CoMSIA (II)	CoMFA	CoMSIA(I)	CoMSIA(II)
1[t]	1.82	2.329	2.222	2.300	0.510	0.400	0.480
2	1.42	1.356	1.378	1.457	−0.06	−0.04	0.040
3	1.45	1.497	1.386	1.290	0.050	−0.06	−0.17
4[t]	2.37	1.377	1.929	1.993	−0.99	−0.44	−0.38
5[t]	1.32	1.801	2.157	2.201	0.480	0.840	0.880
6	1.93	1.547	1.777	1.991	−0.38	−0.15	0.060
7	1.13	1.240	1.092	1.052	0.110	−0.04	−0.08
8	1.87	1.866	1.958	1.954	000	0.090	0.080
9	2.64	2.681	2.599	2.653	0.040	−0.04	0.010
10[t]	2.17	1.508	1.470	1.474	−0.66	−0.70	−0.70
11	2.71	2.845	2.715	2.704	0.130	0.010	−0.01
12	3.31	3.269	3.333	3.327	−0.04	0.020	0.020
13	2.29	2.374	2.301	2.305	0.080	0.010	0.010
14	1.66	1.706	1.761	1.675	0.050	0.100	0.010
15	1.37	1.606	1.454	1.496	0.240	0.080	0.130
16[t]	1.16	1.832	2.335	2.372	0.670	1.180	1.210
17	1.23	1.297	1.174	1.140	0.070	−0.06	−0.09
18	2.46	2.264	2.350	2.314	−0.20	−0.11	−0.15
19	2.2	2.308	2.327	2.220	0.110	0.130	0.020
20	1.33	1.206	1.357	1.276	−0.12	0.030	−0.05
21	2.71	2.754	2.747	2.725	0.040	0.040	0.010
22	1.26	1.304	1.259	1.229	0.040	000	−0.03
23	2.71	2.675	2.686	2.626	−0.04	−0.02	−0.08
24	2.91	2.848	2.868	2.984	−0.06	−0.04	0.070
25	1.26	1.08	1.192	1.159	−0.18	−0.07	−0.10
26	0.75	0.765	0.656	0.752	0.010	−0.09	000
27	0.48	0.765	0.656	0.752	0.280	0.180	0.270
28	1.46	1.287	1.512	1.290	−0.17	0.050	−0.17

[a] t = test set compounds.

CoMFA contour map

The CoMFA steric and electrostatic fields are depicted as contour plots in Fig. 3, where compound **27** is shown to aid in visualization. Green contour indicated regions where increased steric bulk is associated with enhanced activity, and yellow contour regions suggested steric bulk is unfavorable for activity.

The large green contour was found near the plane of the substituted phenyl ring that is attached with a carbonyl group by means of an amide linkage at R$_1$ of compound **25**, indicating that bulky substituents were preferred in this region (Fig. 3). This may be the reason why compounds with bulky phenyl substituents in this area, *e.g.* compounds **2, 3, 5, 7, 14, 15, 16,**
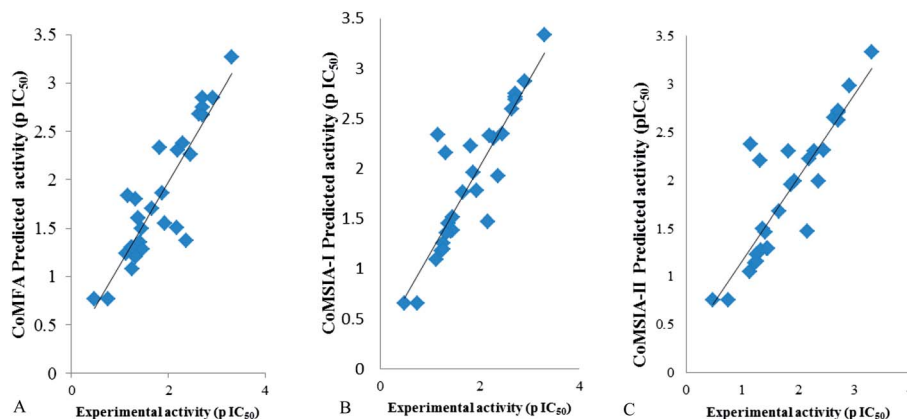

Fig. 2 (A) Correlation between the experimental and CoMFA-predicted activities (pK_i) of compounds. (B) Correlation between the experimental and CoMSIA-I-predicted activities (pK_i) of compounds. (C) Correlation between the experimental and CoMSIA-II-predicted activities (pK_i) of compounds.
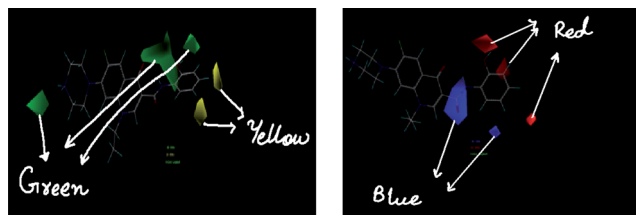
Fig. 3 CoMFA contour maps: green and yellow polyhedra indicate regions where steric bulk will enhance and reduce the anti-inflammatory activity, respectively. Blue and red polyhedra indicate regions where positive charge or negative charge, respectively, will enhance the activity. For an ease of visualization, compound **25** was displayed in the maps.

17, 25, 26, 27 and 28, are more potent molecules. Further, a small green contour at the *ortho* and *meta* positions of this phenyl ring favored the bulkiness. A medium green contour near the substituted piperazine ring suggested that a medium-substituted-piperizinyl ring has greater activity, as seen in compounds 2, 3, 22 and 25. A medium yellow contour is located around the *para* position of the substituted phenyl ring of compound 25, suggesting that groups with low steric factors are

required in this region to increase the activity (Fig. 3). This is possibly the reason as to why compound **4** is less potent.

The CoMFA electrostatic contour plot for highly active compound **25** is displayed in Fig. 3. A blue contour indicated that substituents should be electron deficient for high anti-inflammatory activity, while red color indicated that they should be electron rich for the same. A large blue contour is found overlapping with nitrogen between the carbonyl group and phenyl ring in most of the compounds, indicating that the presence of the nitrogen is not essential but very important for the activity. The red contour surrounding the *ortho*-hydroxyl group substituent on the phenyl ring indicates that greater electron density at this site is important for anti-inflammatory activity, which is clearly supported by the high activity of compounds **20** and **25**. But compounds with electron-rich substituents at the *meta* position of the phenyl ring show poor activity, *e.g.*, compound **18** and **19**, while compounds with electron deficient substituents at the same position show good activity, *e.g.*, compound **16**.

CoMSIA contour maps

The CoMSIA contours maps, derived using steric, electrostatic, hydrogen-bond donor and hydrogen-bond acceptor fields, are
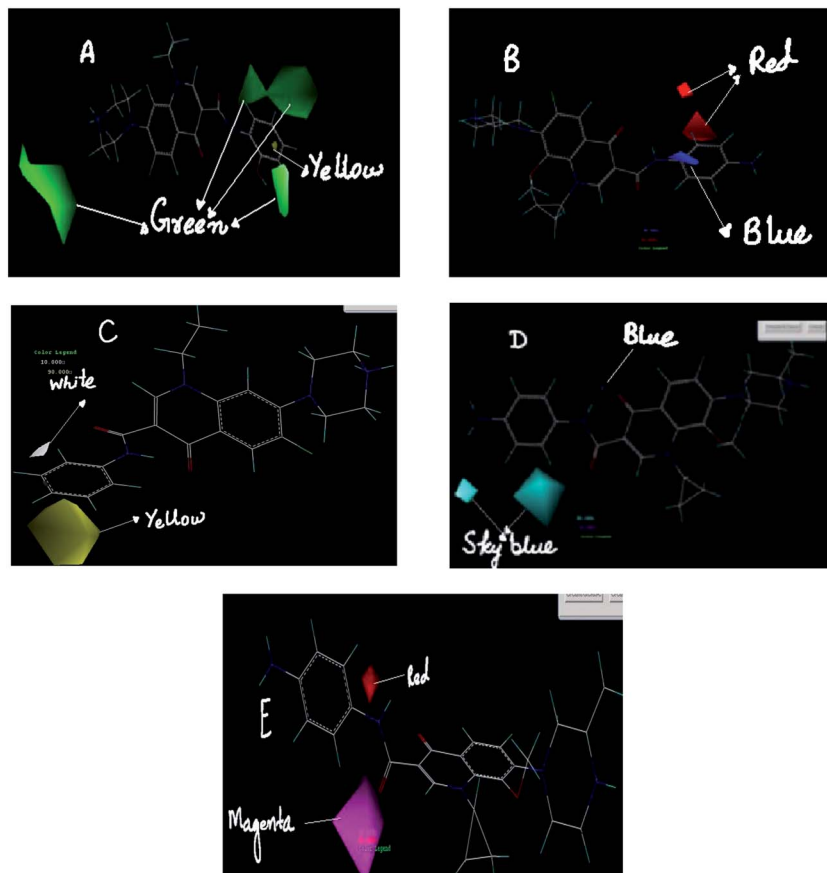
Fig. 4 (A–E) CoMSIA contour maps: compounds 25, 7, 27, 7 & 7 are shown inside the fields A, B,C, D, and E, respectively. Green and yellow polyhedra indicate regions where more steric bulk or less steric bulk, respectively, will enhance the activity. Blue and red polyhedra indicate regions where positive or negative charge, respectively, will enhance the activity. Yellow and white polyhedra indicate regions where hydrophobicity and hydrophilicity, respectively, will enhance the activity. Cyan (sky blue) and blue indicate regions where HB donor increase decreases the activity. Magenta and red polyhedra indicate regions where HB acceptors are favored or disfavored.

presented in Fig. 4A–E. CoMSIA steric and electrostatic contours are more or less similar to those of CoMFA. In resemblance to CoMFA, CoMSIA also showed a large green contour overlapping the plane of the substituted phenyl ring of compound **25** to indicate that bulky substituents were preferred in this region (Fig. 4A). A small yellow contour was found at the *para* position of the phenyl ring. This was the region where bulkier substituents would not be preferred, rendering compound **4**, which has bulkier substituents, less active. Fig. 2B showed the CoMSIA electrostatic fields denoted by red and blue contours. Red contours represented regions where negatively charged substituents are preferred on ligands, and blue contours indicated regions where electron-rich substituents are unfavorable for the activity. The electrostatic fields of CoMSIA as shown in Fig. 4B are also in accordance with the results of CoMFA electrostatic analysis (Fig. 3). The hydrophobic analysis of CoMSIA is depicted in Fig. 4C. The yellow- and white-colored contours represented regions where hydrophobic and hydrophilic substituents are favorable for anti-inflammatory activity. Specifically, a big yellow-colored contour between the *meta* and *para* positions of the phenyl ring indicated that hydrophobicity is favorable for anti-inflammatory activity. This argument is further supported by the high activity of compounds **3**, **5** and **26**. The small white-colored contour near the phenyl ring indicated that hydrophilic substituents on the ring are involved in polar (hydrophilic) interactions with the active site residues. This is supported by the good activity of compound **7**.

Hydrogen-bond donor contour maps from CoMSIA are shown in Fig. 4D. Hydrogen-bond donor-favored regions are represented by cyan (sky blue) contours and unfavorable regions by blue contours. The CoMSIA hydrogen-bond donor contour map showed two cyan contours covering –NH substituents at the amide linkage and at the phenyl ring in compound **7**, suggesting that the substitution of hydrogen-bond donor groups in this region can be expected to improve the activity of the molecule (Fig. 4D), which is why compound **4** is less active than compound **7**. Substituents that act as hydrogen-bond donors may lead to an increase in the activity of the molecule. Fig. 4E displays the hydrogen-bond acceptor contour maps represented by magenta and red contours. Magenta contours indicate regions where hydrogen-bond acceptor substituents on ligands can be favored, and the red ones represent areas where such substituents may be disfavored. In Fig. 4E, a big magenta contour is visible at the ketonic carbonyl functional group of the quinoline ring, which displays the importance of the presence of hydrogen-bond acceptor group for anti-inflammatory activity, and previous studies showed that this group is also essential for antibacterial activity. In Fig. 4E, a small disfavored red contour between the carbonyl group and the phenyl ring may contribute to decreased or moderate activity.

Conclusion

The present study has established reliable CoMFA and CoMSIA models to efficiently guide further modification in molecules for obtaining better drugs. It has provided good statistical results in terms of q^2 and r^2 values. In comparison to CoMFA,

the CoMSIA method was found to provide a slightly better statistical model. However, the reliability of both the models was verified by the compounds in the test set. The 3D-QSAR results revealed some important sites, where steric, electrostatic, hydrophobic, hydrogen-bond donor, and hydrogen-bond acceptor modifications should significantly affect the bioactivities of the compounds. In short, the 3D-QSAR study and experimental biological data suggested that fluroquinolone derivatives show potent anti-inflammatory activity when the hydroxyl group of the carboxylic functional group is replaced by an aromatic primary or secondary amide or ester group. Nitrogen adjacent to the carbonyl group is not essential but very important for activity. At the *ortho* position, electron-rich substituents and hydrogen-bond donors at the *para* position of aromatic ring improved activity, but *meta* electron-rich substituents and hydrophobic substituents at the *para* position of the aromatic ring reduced anti-inflammatory activity. Moreover, a moderate bulky steric group at the piperazine ring improved the activity. These efforts will guide synthetic medicinal chemists to design and synthesize new compounds with increased biological and bifunctional activities in comparison to those of the reported compounds.

Acknowledgements

References

1 A. P. Johnson, M. Warner and D. M. Livermore, Activity of moxifloxacin and other quinolones against pneumococci resistant to first-line agents, or with high-level ciprofloxacin resistance, *Int. J. Antimicrob. Agents*, 2001, **17**, 377–381.

2 I. Fabian, D. Reuveni, A. Levitov, D. Halperin, E. Priel and I. Shalit, Moxifloxacin enhances antiproliferative and apoptotic effects of etoposide but inhibits its proinflammatory effects in THP-1 and Jurkat cells, *Br. J. Cancer*, 2006, **95**, 1038–1046.

3 Y. Azuma, M. Shinohara, W. Pao-Li and K. Ohura, Quinolones alter defense reactions mediated by macrophages, *Int. Immunopharmacol.*, 2001, **1**, 179–187.

4 N. Sultana, A. Naz, B. Khan, M. S. Arayne and M. A. Mesaik, Synthesis, characterization, antibacterial, antifungal and immunomodulating activities of gatifloxacin derivatives, *Med. Chem. Res.*, 2010, **19**, 1210–1221.

5 M. S. Arayne, N. Sultana, U. Haroon, M. A. Mesaik and M. Asif, Synthesis and Biological Evaluations of Enoxacin Carboxamide Derivatives, *Arch. Pharmacal Res.*, 2009, **32**, 967–974.

6 N. Sultana, M. S. Arayne, S. B. S. Rizvi and M. A. Mesaik, Synthesis, Characterization and Biological Evaluation of a Series of Levofloxacin Carboxamide Analogues, *Bull. Korean Chem. Soc.*, 2009, **30**, 2294–2298.

7 M. A. Lill, Multi-dimensional QSAR in drug discovery, *Drug Discovery Today*, 2007, **12**, 1013–1017.

8 B. Llorente, F. Leclerc and R. Cedergren, Using SAR and QSAR Analysis to Model the Activity and Structure of the Quinolone-DNA Complex, *Bioorg. Med. Chem.*, 1996, **4**, 61–71.

9 C. Walsh, *Antibiotics, Actions, Origins, Resistance*, ASM Press, Harvard Medical School, Boston, 2003.

10 A. R. Ronald and D. E. Low, *Fluoroquinolones Antibiotics*, Birkhäuser Verlag, Basel, 2003.

11 R. D. Cramer, D. E. Patterson and J. D. Brounce, Comparative molecular field analysis (COMFA). Effect of shape on binding of steroid to carrier proteins, *J. Am. Chem. Soc.*, 1988, **110**, 5959–5967.

12 T. K. Chang, C. Y. Chen, H. N. Wan, W. C. Li, L. C. Lung, L. Y. Ching, L. Minyong and W. Binghe, A comparison of different electrostatic potentials on prediction accuracy in CoMFA and CoMSIA studies, *Eur. J. Med. Chem.*, 2010, **45**, 1544–1551.

13 M. C. Clark, R. D. Cramer and N. V. O. Bosch, Validation of the general purpose tripos 5.2 force field, *J. Comput. Chem.*, 1989, **10**, 982–1012.

14 V. Srivastava, S. P. Gupta, M. I. Siddiqi and B. N. Mishra, 3D-QSAR studies on quinazoline antifolate thymidylate synthase inhibitors by CoMFA and CoMSIA models, *Eur. J. Med. Chem.*, 2010, **45**, 1560–1571.

15 G. Klebe and U. Abraham, Comparative Molecular Similarity Index Analysis (CoMSIA) to Study Hydrogen Bonding Properties and to Score Combinatorial Libraries, *J. Comput.-Aided Mol. Des.*, 1999, **13**, 1–10.

16 A. D. Andricopulo and C. A. Montanari, Structure activity relationships for the design of small molecule inhibitors, *Mini-Rev. Med. Chem.*, 2005, **5**, 585–593.

17 R. V. C. Guido, G. Oliva, C. A. Montanari and A. D. Andricopulo, Structural basis selective inhibition of trypanosomatid glyceraldehyde-3-phosphate dehydrogenase: molecular docking and 3D QSAR studies, *J. Chem. Inf. Model.*, 2008, **48**, 918–929.

18 *Cerius² Life Sciences, version 4.5*, Accelrys, San Diego, CA, 2000.

19 N. Thomas and F. W. Donald, *Medicinal Chemistry*, Oxford University Press, 3rd edn, 2005, pp. 335–337.

20 H. Heijerman, Infection and inflammation in cystic fibrosis: a short review, *J. Cystic Fibrosis*, 2005, **4**(2), 3–5.

21 D. Kube, U. Sontich, D. Fletcher and P. B. Davis, Proinflammatory cytokine responses to P. aeruginosa infection in humanairway epithelial cell lines, *Am. J. Physiol.: Lung Cell. Mol. Physiol.*, 2001, **280**, L493–L502.

22 C. M. Oliphant and G. M. Green, Quinolones: A Comprehensive Review, *Am. Fam. Physician*, 2002, **65**(3), 455–464.

23 A. Dalhoff and I. Shalit, Immunomodulatory effects of quinolones, *Lancet Infect. Dis.*, 2003, **3**(6), 359–371.

24 N. Sultana, A. Naz, M. S. Arayne and M. A. Mesaik, Synthesis, characterization, antibacterial, antifungal and immunomodulating activities of gatifloxacin–metal complexes, *J. Mol. Struct.*, 2010, **969**, 17–24.

25 H. Urooj, M. H. Zuberi, M. S. Arayne and N. Sultana, New Improved Quinolone Derivatives Against Infection, Biochemistry, Genetics and Molecular Biology, in *A Search for Antibacterial Agents*, ed. B. Varaprasad, September 19 2012, ch. 12, DOI: 10.5772/46048, ISBN 978-953-51-0724-8, published, under CC BY 3.0 license.

26 D. C. Hooper, Emerging mechanisms of fluoroquinolone resistance, *Emerging Infect. Dis.*, 2001, **7**(2), 337–341.

27 D. E. Karageorgopoulos, K. P. Giannopoulou, A. P. Grammatikos, G. Dimopoulos and M. E. Falagas, Fluoroquinolones compared with β-lactam antibiotics for the treatment of acute bacterial sinusitis: a meta-analysis of randomized controlled trials, *Can. Med. Assoc. J.*, 2008, **178**(7), 845–854, DOI: 10.1503/cmaj.071157.

28 N. Sultana, M. S. Arayne, A. Naz and M. A. Mesaik, Identification of anti-inflammatory and other biological activities of 3-carboxamide, 3-carbohydrazide and ester derivatives of gatifloxacin, *Chem. Cent. J.*, 2013, **7**, 6.

29 H. Tokushige, S. Yokogaki and H. Naka, Cytokine Production Inhibitors, US patent application Publ. US 2003/0176444A1, 18 Sep 2003.

30 *ChemDraw, Cambridge Software Corporation, 64-71.5.3 version*, 2004.

31 Molecular Operating Environment (MOE), 2012.10; Chemical Computing Group Inc., 1010 Sherbooke St. West, Suite #910, Montreal, QC, Canada, H3A 2R7, 2012.

32 G. Wolber, T. Seidel, F. Bendix and T. Langer, Molecule-pharmacophore super-positioning and pattern matching in computational drug design, *Drug Discovery Today*, 2008, **13**, 23–29.

33 K. M. Honorio, R. C. Garratt, I. Polikatpov and A. D. Andricopulo, 3D QSAR comparative molecular field analysis on non-steroidal farnesoid X receptor activators, *J. Mol. Graphics Modell.*, 2007, **25**, 921–927.

34 C. H. Andrade, L. B. Salum, K. F. M. Pasqualoto, E. I. Ferreira and A. D. Andricopulo, Three Dimensional Quantitative Structure–Activity Relationships for a Large Series of Potent Antitubercular Agents, *Lett. Drug Des. Discovery*, 2008, **5**, 377–387.

35 A. M. Doweyko, 3D-QSAR illusions, *J. Comput.-Aided Mol. Des.*, 2004, **18**, 587–596.

36 C. A. Lipinski, F. Lombardo, B. W. Dominy and P. J. Fenney, Experimental and computational approaches to estimate solubility and permeability in drug discovery and development settings, *Adv. Drug Delivery Rev.*, 2001, **46**, 3–26.

37 A. Tropsha, Application of predictive QSAR models to database mining, in *Chemoinformatics in Drug Discovery*, ed. T. Oprea, Wiley-VCH, Weinheim, 2005.